Observation of the Charge Symmetry Breaking $d + d \rightarrow {}^4\mathrm{He} + \pi^0$ Reaction Near Threshold

E. J. Stephenson,[1] A. D. Bacher,[1,2] C. E. Allgower,[1] A. Gårdestig,[3] C. M. Lavelle,[1] G. A. Miller,[4] H. Nann,[1,2] J. Olmsted,[1] P.V. Pancella,[5] M. A. Pickar,[6] J. Rapaport,[7] T. Rinckel,[1] A. Smith,[8] H. M. Spinka,[9] and U. van Kolck[10,11]

[1]*Indiana University Cyclotron Facility, Bloomington, Indiana 47408, USA*
[2]*Department of Physics, Indiana University, Bloomington, Indiana 47405, USA*
[3]*Indiana University Nuclear Theory Center, Bloomington, Indiana 47408, USA*
[4]*Department of Physics, University of Washington, Seattle, Washington 98195, USA*
[5]*Physics Department, Western Michigan University, Kalamazoo, Michigan 49008, USA*
[6]*Department of Physics and Astronomy, Minnesota State University at Mankato, Mankato, Minnesota 56001, USA*
[7]*Department of Physics and Astronomy, Ohio University, Athens, Ohio 45701, USA*
[8]*Physics Department, Hillsdale College, Hillsdale, Michigan 49242, USA*
[9]*Argonne National Laboratory, Argonne, Illinois 60439, USA*
[10]*Department of Physics, University of Arizona, Tucson, Arizona 85721, USA*
[11]*RIKEN BNL Research Center, Brookhaven National Laboratory, Upton, New York 11973, USA*
(Received 9 May 2003; published 2 October 2003)

We report the first observation of the charge symmetry breaking $d + d \rightarrow {}^4\mathrm{He} + \pi^0$ reaction near threshold. Measurements using a magnetic channel (gated by two photons) of the ${}^4\mathrm{He}$ scattering angle and momentum (from time of flight) permitted reconstruction of the π^0 "missing mass," the quantity used to separate ${}^4\mathrm{He} + \pi^0$ events from the continuum of double radiative capture ${}^4\mathrm{He} + \gamma + \gamma$ events. We measured total cross sections for neutral pion production of 12.7 ± 2.2 pb at 228.5 MeV and 15.1 ± 3.1 pb at 231.8 MeV. The uncertainty is dominated by statistical errors. These cross sections arise fundamentally from the down-up quark mass difference and quark electromagnetic effects that contribute in part through meson mixing (e.g., $\pi^0 - \eta$) mechanisms.

DOI: 10.1103/PhysRevLett.91.142302 PACS numbers: 24.80.+y, 24.85.+p, 25.10.+s, 25.45.–z

Charge symmetry is the symmetry of the quantum chromodynamic Lagrangian under the interchange of equal-mass up and down quarks [1,2]. This symmetry is broken by the different masses of the down and up quarks ($m_d > m_u$) and by their electromagnetic interactions. The combination of these two mechanisms leads, for example, to the neutron being heavier than the proton. Within the framework of chiral effective field theory [3,4], additional experimental information on the relative contributions of these two mechanisms to charge symmetry breaking (CSB) must, in leading order, come from pion-nucleon scattering. Direct experimental evidence is restricted to elastic scattering and charge exchange experiments with low-energy charged pions where the interpretation is complicated by corrections for the neutron-proton mass difference and electromagnetic interactions between the pions and nucleons [5,6]. Reactions in which a π^0 is emitted after being created by one nucleon and rescattered by a second are particularly clean. One example of such a CSB process is the measurement of a forward-backward asymmetry in the cross section for the $n + p \rightarrow d + \pi^0$ reaction [7].

The $d + d \rightarrow {}^4\mathrm{He} + \pi^0$ reaction violates the conservation of isospin because the pion has isospin one while both the deuteron and ${}^4\mathrm{He}$ have isospin zero. More specifically, it violates charge symmetry, which is a rotation by $\pi/2$ about the y axis in charge space that interchanges up and down quarks. (Isospin conservation is invariance under any rotation.) The π^0, whose wave function is odd under the interchange of down and up quarks, should not be produced from an initial state with charge symmetry even (in this case self-conjugate). The amplitude for CSB is weaker than a similar charge symmetry conserving amplitude by about $1/300$, roughly the ratio of the quark mass difference to the nucleon mass. This suggests a $d + d \rightarrow {}^4\mathrm{He} + \pi^0$ total cross section, which depends only on a CSB amplitude, that is as small as tens of picobarns.

Several searches for the $d + d \rightarrow {}^4\mathrm{He} + \pi^0$ reaction have produced only upper limits [8]. A positive report at a deuteron energy of 1.1 GeV [9] has been questioned because the experiment did not clearly distinguish the photons from π^0 decay from photons that could have been produced by the double radiative capture $d + d \rightarrow {}^4\mathrm{He} + \gamma + \gamma$ process. This isospin-allowed process was calculated to be of the same order as the reported cross section [10]. A further search that could clearly distinguish between these two reactions was therefore warranted.

We chose to look for the $d + d \rightarrow {}^4\mathrm{He} + \pi^0$ reaction just above its threshold at 225.5 MeV to avoid other pion producing channels and to take advantage of the clean experimental conditions afforded by the Indiana University Cyclotron Facility's electron-cooled storage ring. A 6° bend located in one section of the ring provided a site where ${}^4\mathrm{He}$ nuclei, produced in a narrow forward cone just above threshold, could be separated from the circulating deuteron beam. By placing a gas jet target sufficiently upstream of the 6° magnet, it became possible to cover a large solid angle with two arrays of Pb glass detectors that would be selectively sensitive to photons from the target region.

The layout of the experiment is shown in Fig. 1, with the major features being two arrays of Pb glass detectors stacked on the left and right sides of the gas target box, the 6° separation magnet, and a magnetic channel consisting of a septum magnet to steer the ^{4}He nuclei away from the downstream ring quadrupole magnets and a quadrupole triplet to confine the ^{4}He nuclei within the acceptance of the detectors at the end of a long, evacuated drift length.

For some $^4\mathrm{He} + \pi^0$ events, the ^{4}He nucleus and both π^0 decay photons could be recorded. Parts of the solid angle above and below the target were required for differential pumping of the jet target volume. Kinematic constraints just above threshold yield very similar photon opening angles and energies for $^4\mathrm{He} + \pi^0$ and $^4\mathrm{He} + \gamma + \gamma$ events. Separation of these two reactions relied on measuring the ^{4}He momentum vector using time of flight in the channel for the longitudinal component and scattering angle for the transverse component. The flight time was measured from the first plastic scintillation detector (ΔE1) to the second (ΔE2) at the end of the channel 5.73 m away. A third scintillator (E) in which the ^{4}He nuclei stopped was required for an event trigger along with the absence of any signal in two additional scintillators (V1 and V2). Pulse-height correlations among the trigger scintillators cleanly separated ^{4}He events from $Z = 1$ particles. Pb glass information was not used in the trigger. The scattering angle of the ^{4}He was recorded by a multiwire proportional chamber (WC1). Two additional chambers (WC2 and WC3) tracked each ^{4}He nucleus through the channel. From the ^{4}He momentum and the assumption of a two-body final state, it is possible to calculate the missing mass. Double radiative capture events produce a broad distribution of mass values up to a kinematic limit that depends on the beam energy, rather than a peak at the π^0 mass.

The isospin-allowed $p + d \rightarrow {}^3\mathrm{He} + \pi^0$ reaction was used to commission the detector system. The calculation of ^{3}He (and later ^{4}He) momentum from channel time of flight used a model to describe the energy loss (scaled from Janni [11]) of the ^{3}He passing through the channel detectors and vacuum windows. The time offsets for each photomultiplier associated with the ΔE1 and ΔE2 detectors were adjusted empirically during the subsequent data analysis. For ^{3}He energies close to threshold and runs lasting several hours, a π^0 mass resolution as small as FWHM $= 240$ keV was obtained.

For $p + d \rightarrow {}^3\mathrm{He} + \pi^0$ events in which both π^0 photons were recorded, photon energies were taken to be the sum of Pb glass energies starting with the detector recording the highest energy deposition and including its eight nearest neighbors. The average photon energy was 70 MeV; the detectors were between 12 and 16 radiation lengths thick to the photons. With summed energies above a threshold chosen to remove most random events and with Pb glass timing in the correct range relative to the channel trigger, the measured efficiency for detecting the two π^0 decay photons was 0.360 ± 0.001, a value that reflects gaps in solid angle coverage. Simulations using the GEANT Monte Carlo program library [12] and the known π^0 angular distribution [13] reproduced the Pb glass spectral energy shape and agreed with the measured efficiency to ± 0.01. This simulation was used to obtain the changes in Pb glass efficiency between the $p + \mathrm{d} \rightarrow {}^3\mathrm{He} + \pi^0$ commissioning run and production running for $d + d \rightarrow {}^4\mathrm{He} + \pi^0$ due to alterations of the kinematics and center-of-mass angular distribution (assuming the

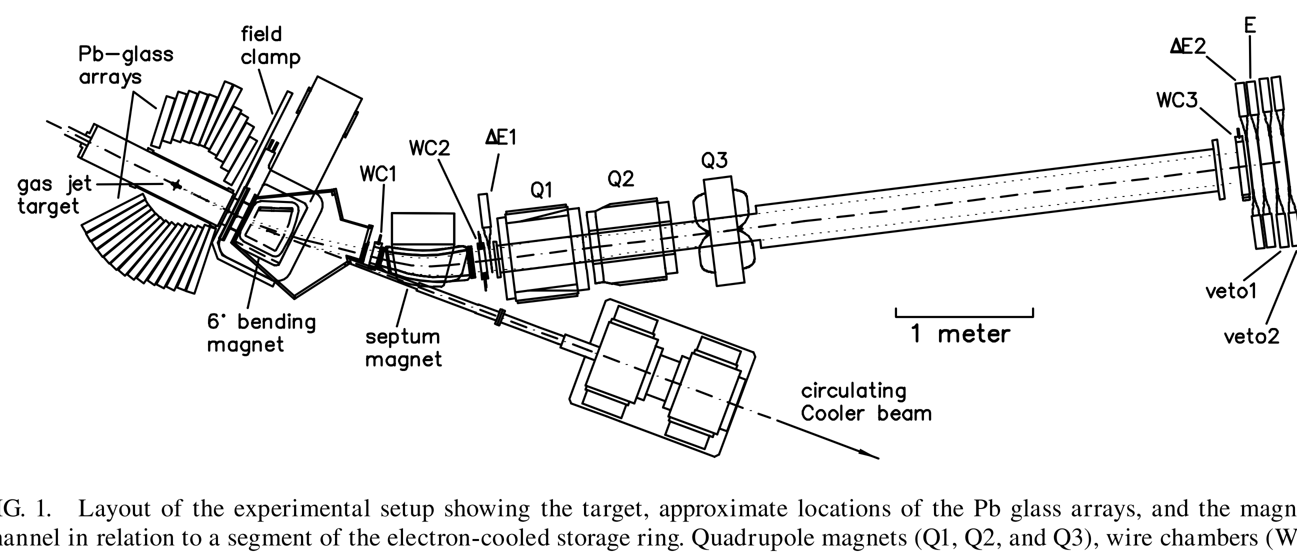

FIG. 1. Layout of the experimental setup showing the target, approximate locations of the Pb glass arrays, and the magnetic channel in relation to a segment of the electron-cooled storage ring. Quadrupole magnets (Q1, Q2, and Q3), wire chambers (WC1, WC2, and WC3), and scintillation trigger (ΔE1, ΔE2, and E) and veto (V1 and V2) detectors are shown. The luminosity detectors are small and consequently are omitted here.

$d + d \to {}^4\text{He} + \pi^0$ cross section to be isotropic). Gains for the Pb glass detectors were calibrated using cosmic ray muons. This calibration operated continuously during commissioning and production running.

The size of the ^{3}He opening angle cone for $p + d \to {}^3\text{He} + \pi^0$ calibrated the incident proton energy. Several determinations at slightly different energies were combined by using the frequency of the rf voltage that maintained the beam bunching to calculate the circumference of the storage ring, yielding a value of 86.786 ± 0.003 m that was consistent over time. This calibration was used subsequently for the deuteron beam energy.

The deuterium target was made by directing deuterium gas from a glass nozzle cooled to about 40 K across the circulating storage ring beam (~ 2 mm wide). The gas flow was adjusted so that the beam lifetime was close to 100 s with the rf voltage and electron cooling on, a value that gave the largest data production rate. The circulating beam current was as large as 2 mA.

The luminosity (product of beam flux and intercepted target thickness) was determined through a separate calibrated monitoring system. For this we used $d + d$ elastic scattering in the vicinity of $\theta_{\text{c.m.}} = 90°$ by placing two scintillator detectors at 44° on each side of the beam. The product of $d + d$ differential cross section and solid angle for this system was measured in a separate experiment using a molecular HD target. Additional scintillators were added to observe $d + p$ elastic scattering. Using known $d + p$ cross sections and the equality of $d + p$ and $d + d$ luminosities for an HD target, we obtained the $d + d$ calibration. Cross sections for $d + p$ elastic scattering in our energy range have recently become available [14] with an absolute normalization error of 5.5%. The scintillation detectors provided particle identification information to separate breakup and other backgrounds. An additional position-sensitive silicon detector used to record recoil nuclei from small-angle scattering provided a measurement of the jet target profile as it intercepted the beam. This information was used to make corrections to the scintillator acceptance geometry for both the $d + p$ and $d + d$ elastic scattering processes, and to track changes between calibration and production running. The average luminosity during production was $2.9 \times 10^{31}/(\text{cm}^2\,\text{s})$.

Candidate $d + d \to {}^4\text{He} + \pi^0$ events were required to have the correct pulse height in the three trigger scintillators (ΔE1, ΔE2, and E), usable wire chamber information, and photon signals in both the left and right Pb glass arrays with an energy sum above threshold and timing coincident with ^{4}He events in the channel. For each candidate event the missing mass was calculated. The results were accumulated into a spectrum, as shown in Fig. 2. Investigations of the quality of the data set showed that random background was essentially removed (≤ 1 event/spectrum); thus we should interpret these results as arising only from π^0 production and double radiative capture.

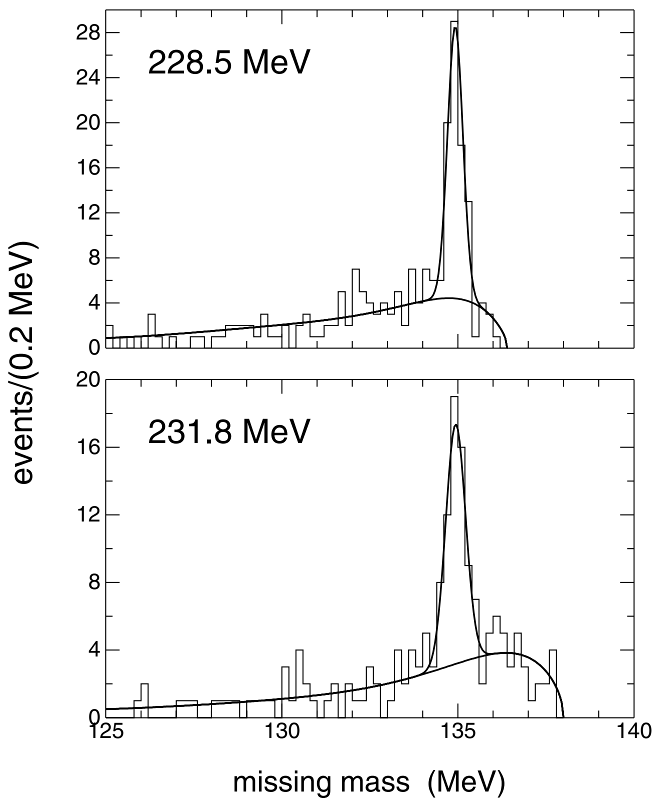

FIG. 2. Histograms of the candidate events at the two deuteron bombarding energies as a function of their missing mass value. The smooth curves show the reproduction of these histograms with a Gaussian peak and a continuum.

Production running started at 228.5 MeV, an energy chosen because the half-angle of the ^{4}He forward cone (1.2°) was expected to fit well inside the channel acceptance. Over the much longer $d + d \to {}^4\text{He} + \pi^0$ production running times, drifts in the time-of-flight measurement became more of a problem, despite efforts to track timing changes by monitoring other particles going through the channel. The width of the missing mass peak was FWHM = 510 keV, as seen in the top panel of Fig. 2. This meant that the peak was not well separated from the $^4\text{He} + \gamma + \gamma$ kinematic upper limit of 136.4 MeV. Below the peak, the flux we would attribute to double radiative capture is attenuated by the acceptance boundaries of the channel, increasing the ambiguity of its shape. The decision was made to complete production running at the higher energy of 231.8 MeV (1.75° cone) with a kinematic end point of 138.0 MeV even though an additional 10% of the π^0 events would be lost in the channel. The result shown in the lower panel of Fig. 2 still has a broad peak (FWHM = 660 keV) but there is now a clear distribution of double radiative capture events on either side.

The spectra of Fig. 2 were modeled with a Gaussian peak and a continuum. The continuum shape was obtained from the distribution in missing mass of all ^{4}He events (rate about 10^3 higher than for candidate events alone) reduced by the ratio of the calculated double radiative capture cross section [15] to the phase space value, both of which are a function of missing mass. These ^{4}He events without coincident photons, which may have originated from (d, ^{4}He) reactions on residual gas and storage ring structures, were broadly distributed in energy and angle, and were used as an estimate of the product of phase space and channel acceptance. The continuum curves in Fig. 2 are a smooth representation of this shape. The centroids of the Gaussian peaks have a fitting error of less than 60 keV and are consistent with the π^0 mass. Events in the peak appear to be isotropically distributed in the center of mass as determined by their distribution in scattering angle and time of flight.

The 66 and 50 $^4\mathrm{He} + \pi^0$ events recorded at the two energies of 228.5 and 231.8 MeV lead to total cross section values of 12.7 ± 2.2 and 15.1 ± 3.1 pb, respectively, including a 6.6% normalization error for all systematic effects. Corrections at the two energies included Pb glass efficiency (0.34 and 0.32), trigger losses (0.94 and 0.96 for random vetoes), system livetime (0.95 and 0.94), wire chamber efficiency (0.93 and 0.95), and other channel losses from acceptance and multiple scattering (0.95 and 0.81). These cross sections are consistent with being proportional to $\eta = p_\pi/m_\pi$ with a slope of $\sigma_{\mathrm{TOT}}/\eta = 80 \pm 11$ pb. The integral of the double radiative capture process for the 2 MeV range just below the kinematic limit is 6.9 ± 0.9 and 9.5 ± 1.4 pb at the two energies. This is more than twice the model predictions [15].

These results provide the first unambiguous measurement of the $d + d \rightarrow {}^4\mathrm{He} + \pi^0$ cross section as well as that for the competing double radiative capture process. A detailed interpretation of our results will require a careful consideration of different CSB reaction mechanisms. On the basis of chiral power counting arguments, the leading terms are expected to be [16] the one-body amplitude and $\pi + N$ scattering [3]. The size of the one-body amplitude may be estimated from $\pi^0 - \eta$ mixing [17]. Preliminary plane wave calculations [16] suggest that $\pi^0 - \eta$ mixing may be important because all four nucleons contribute coherently. This is particularly true if the η is produced by two nucleons via the exchange of a heavy meson, as in $p + p \rightarrow p + p + \pi^0$ [18]. This chiral contact term can also involve contributions from $\pi^0 - \eta'$ mixing as well as $\rho^0 - \omega$ mixing in the heavy meson exchange. The effects of pion scattering are also expected to be enhanced by the initial state $d + d$ interactions [16]. Preliminary estimates show that electromagnetic effects are very small.

Both $\pi^0 - \eta$ mixing and CSB $\pi + N$ scattering are also important in producing an asymmetry about 90° in the $n + p \rightarrow d + \pi^0$ reaction [4], with the latter determining the sign of the asymmetry. Calculations now underway should allow the study of these CSB mechanisms based on the combined experimental results. Since nuclear CSB arises fundamentally from the quark mass difference and electromagnetic effects, this new experimental information will help to separate each contribution and greatly enhance efforts to relate the hadronic matrix elements to the underlying QCD theory.

We would like to thank V. Anferov, G. P. A. Berg, B. Chujko, J. Doskow, G. East, C. C. Foster, W. Fox, D. Friesel, T. Hall, C. J. Horowitz, A. Kuznetsov, V. Medvedev, H. O. Meyer, D. Patalahka, R. E. Pollock, A. Prudkoglyad, S. Shastry, T. Sloan, K. Solberg, J. Vanderwerp, and B. von Przewoski for their contributions to the preparation of this experiment. Our work was supported in part by the National Science Foundation Grants No. PHY-97-22538, No. PHY-98-02872, No. PHY-00-70368, and No. PHY-01-00348, and the U.S. Department of Energy Grant No. DE-AC02-98CH10886.

[1] G. A. Miller, B. M. K. Nefkens, and I. Šlaus, Phys. Rep. **194**, 1 (1990).
[2] G. A. Miller and W. T. H. van Oers, in *Symmetries and Fundamental Interactions in Nuclei*, edited by W. C. Haxton and E. M. Henley (World Scientific, Singapore, 1995), p. 127, and references therein.
[3] U. van Kolck, Few-Body Syst., Suppl. **9**, 444 (1995).
[4] U. van Kolck, J. A. Niskanen, and G. A. Miller, Phys. Lett. B **493**, 65 (2000).
[5] W. R. Gibbs, Li Ai, and W. B. Kaufmann, Phys. Rev. Lett. **74**, 3740 (1995).
[6] C. Matsinos, Phys. Rev. C **56**, 3014 (1997).
[7] A. K. Opper *et al.*, arXive:nucl-ex/0306027.
[8] J. Banaigs *et al.*, Phys. Rev. Lett. **58**, 1922 (1987), and references therein.
[9] L. Goldzahl, J. Banaigs, J. Berger, F. L. Fabbri, J. Hüfner, and L. Satta, Nucl. Phys. A **533**, 675 (1991).
[10] D. Dobrokhotov, G. Fäldt, A. Gårdestig, and C. Wilkin, Phys. Rev. Lett. **83**, 5246 (1999).
[11] J. F. Janni, At. Data Nucl. Data Tables **27**, 147–529 (1982).
[12] GEANT program library, http://wwwinfo.cern.ch/asdoc/geant.html3/geantall.html.
[13] M. A. Pickar *et al.*, Phys. Rev. C **46**, 397 (1992).
[14] K. Ermisch *et al.*, arXive:nucl-ex/0308012; K. Ermisch, Ph.D. thesis, Rijkuniversiteit Groningen, 2003.
[15] Made by A. Gårdestig based on Ref. [10].
[16] A. Fonseca, A. Gårdestig, C. Hanhart, C. J. Horowitz, G. A. Miller, J. A. Niskanen, A. Nogga, and U. van Kolck (to be published).
[17] S. A. Coon and B. M. Preedom, Phys. Rev. C **33**, 605 (1986).
[18] T.-S. H. Lee and D. O. Riska, Phys. Rev. Lett. **70**, 2237 (1993).